SAFETY AND THERMO-MECHANICAL PERFORMANCE OF METALLIC HELICAL CRUCIFORM FUEL IN LIGHT-WATER COOLED SMALL MODULAR REACTORS

Y. CHOI, K. SHIRVAN
Department of Nuclear Science and Engineering, Massachusetts Institute of Technology
77 Massachusetts Ave, 02139 Cambridge MA – United States of America

ABSTRACT

This study investigates the safety and thermo-mechanical performance of metallic helical cruciform fuel (HCF) for light-water cooled small modular reactors (SMRs). U-50wt.%Zr (U-50Zr) alloy is used as a fuel material which has higher Zr content compared to traditional metallic fuel which was used in fast reactor applications. As the name implies, HCF has a cruciform shape and is helically twisted, giving a larger heat transfer area than a cylindrical fuel. For the safety performance study, CFD simulation with Eulerian-based two-fluid approach is used for hot channel analysis and critical heat flux (CHF) assessment. Compared with cylindrical rod geometry, the HCF channel shows lower CHF, indicating that it has more room for power uprate under the same power and flow conditions. For the thermo-mechanical study, finite element-based fuel performance analysis is carried out for a hot fuel pin. First, given that there's high uncertainty in using current metallic fuel models for Zr-rich fuel, a sensitivity study is performed to see the impact of each model on the main figure of merits (FOMs). In addition to that, the fuel volumetric swelling model is modified to consider different fission gas behaviours depending on uranium phases. Lastly, a comparison between U-50Zr HCF and UO_2 cylindrical fuel is carried out through hot fuel pin analysis where metallic HCF shows much lower fuel operating temperature but higher cladding stress.

1. Introduction

As the commercial viability of small modular reactors (SMRs) has been challenged due to a lack of economy of scale and low power density, innovation in fuel design can be a promising solution to improve the competitiveness of SMRs in the energy market. Massachusetts Institute of Technology (MIT) has been working on a design study based on Lightbridge Corporation's Helical Cruciform Fuel (HCF) concept [1], for a 250 MWth NuScale Power Module as a reference plant. HCF contains U-50Zr alloy as a fuel material and as the name implies, it has a cruciform shape and is helically twisted. A detailed description of the fuel is given in the following section. The advantages of HCF include a low fuel operating temperature driven by the higher thermal conductivity of metallic fuel. In addition, since the fuel heat transfer area is about 35 % larger than a conventional cylindrical fuel for the same volume, the heat flux between the cladding surface and coolant is lower in HCF geometry which implies potential power uprate.

The previous neutronic study [2] performed a two-dimensional NuScale core design using a Monte Carlo code Serpent, and determined a fuel enrichment (~15 %) to achieve the target fuel cycle and the burnable absorber material for reactivity control in the displacer region. The goal of this study is to investigate the safety and thermo-mechanical performance of HCF and compare it with a conventional cylindrical UO_2 fuel. A commercial computational fluid dynamics (CFD) software STAR-CCM+ [3] is used for safety performance study to investigate thermal-hydraulic behaviours in hot channels and for a boiling crisis. For a thermo-mechanical analysis, a finite element-based fuel performance code BISON [4] is used. The result of the sensitivity study on metallic fuel models in BISON is introduced and the hot fuel pin analysis result for

both U-50Zr HCF and cylindrical UO_2 fuel is followed. The detailed simulation setup including computational meshes and models is described in the following result sections.

2. Helical Cruciform Fuel

As shown in Fig 1, HCF consists of a central displacer, fuel, and cladding where U-50Zr alloy is used as a fuel, Zr-1%Nb alloy as a cladding, and a displacer will be potentially filled with burnable absorbers such as zirconium-diboride. The fuel width is 1.26 cm which is identical to the fuel pitch of UO_2 fuel and the twist pitch which is a length in which the fuel is 360-degree fully twisted is 50 cm.
HCF targets to operate in the δ-UZr_2 phase (δ-phase) marked in Fig 1. One of the advantages of having higher Zr content is reduced irradiation-induced swelling and a lower chance of fission gas release compared to U-rich U-Zr alloy [5]. HCF has several additional advantages compared to conventional UO_2 fuel. First, metallic fuel has high thermal conductivity which enables lower operating temperature. At the low fuel operating temperature, fission gases behave like solid fission products and have significantly less mobility. Furthermore, as mentioned above, HCF has about 35 % larger heat transfer area due to the twisted geometry. The main benefit from this for SMRs like NuScale is the likely higher critical heat flux (CHF) margin, which can potentially open the doors to power uprate. Lastly, the fuels are self-spacing by contacting each other as shown in Fig 1, eliminating the spacer grids, leading to lower pressure drop. On the downside, HCF will require higher enrichment (~15 %) to compensate for the low initial fissile loading and its failure modes and temperature limits are not fully understood.

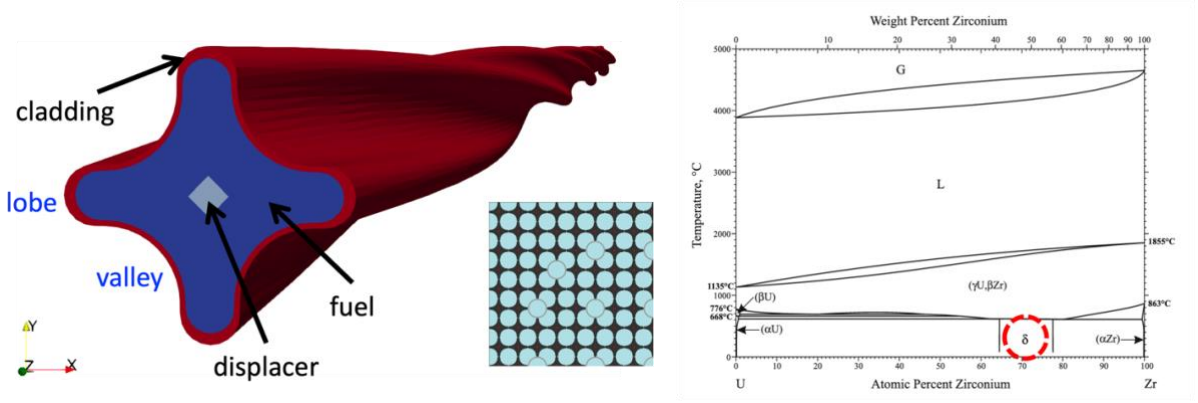

Fig 1. HCF geometry (left) and U-Zr phase diagram [6] (right)

3. Safety performance analysis

3.1 Problem setup

A full height (2 m) single channel geometry is used for safety performance analysis where a fuel rod is modelled as a wall boundary of the fluid domain. The channel pitch for cylindrical fuel is 1.26 cm while that for HCF is 1.36 cm since a small 0.5 mm gap between the wall surface and symmetry plane is placed to avoid a singularity. Given that the assumed twist pitch of HCF is 50 cm, the fuel fully rotates 4 times in a 2 m height channel. The geometrical comparison between the two channels is summarized in Tab 1. As to meshing, the final meshes have a base size of 0.5 mm and the aspect ratio is equal to 1. The near-wall prism layer mesh has a thickness of 0.5 to 0.6 mm and the average wall y+ of both channels which represents the distance from the first grid cell to the surface wall is around 90. This high y+ approach is chosen since the finer prism layer with y+ < 10 results in instability in the two-phase flow solver. The mesh sensitivity study was performed on the bulk mesh and the mesh

refinement (1 mm, 0.75 mm, and 0.5 mm) in the bulk region showed a maximum 5 % difference in pressure drop, which is acceptable in the design evaluation stage. The final mesh configuration is shown in Fig 2.

	CF	HCF	Unit
Pitch	1.26	1.36	cm
Flow area	0.8779	1.2050	cm^2
Fuel surface area	596.75	802.20	cm^2
Channel height	2	2	m

Tab 1: Channel geometry comparison of Cylindrical Fuel (CF) with HCF

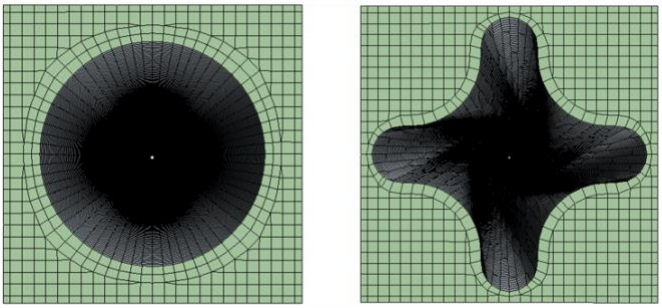

Fig 2. Computational mesh – CF channel (left) and HCF channel (right)

In nuclear reactor applications, the Eulerian-based two-fluid model is widely used in subcooled boiling simulation due to the dispersed nature of the vapor bubbles [7]. This model is implemented as the Eulerian Multiphase (EMP) model in STAR-CCM+ and it requires a set of closure relations for interfacial mass, momentum, and energy transfer as well as wall boiling. Under the Consortium for Advanced Simulation of Light Water Reactors (CASL) program funded by the U.S. Department of Energy, the DNB simulation using this approach was extensively investigated. In this study, the closure selection refers to the CASL's boiling closure selection for DNB application [8] as they are relatively robust and validated against experimental measurements. The closures used in this study are listed in Tab 2. This set of closure relations is validated against the Bartolomei experiment which measured void fraction and wall temperature in subcooled boiling conditions. For a detailed description of each model, [8] can be referred to. For turbulence modeling, a realizable k-ε model with two-layer all y+ wall treatment is used for both liquid and vapor phases. Lastly, regarding the simulation conditions, the inlet mass flux is 771.14 kg/m^2-sec, pressure is 13.8 MPa and pin power is 35.755 kW with the axial power profile.

Parameter	Closure
Interfacial momentum/energy transfer	
Lift force	Sugrue with Podowski near wall adjustment
Drag force	Tomiyama et al. with contamination
Turbulent dispersion force	Turbulent dispersion Pr=1.0
Wall lubrication force	Lubchenko
Liquid phase condensate	Kim-Park
Vapor phase condensate	Nu=26
Interaction area density	Symmetric
Interaction length scale	S-gamma with Sauter mean diameter
Wall bubble nucleation	
Nucleation site density	Modified Li et al.

Bubble departure diameter	Kocamustafaogullari
Bubble departure frequency	Cole
Wall transient (quenching)	
Bubble-induced fraction	Kurul-Podowski
Bubble-induced HTC	Del Valle-Kenning

Tab 2: Two-fluid model closure selection

3.2 Hot channel analysis

First, a steady-state hot channel analysis is performed for both fuel geometries to understand the thermal-hydraulic behaviour under the most limiting channel during a normal operation. A steady state in STAR-CCM+ is determined by observing an exit flow quality, exit void fraction, maximum local void fraction, and volume-averaged liquid velocity with an asymptotic limit (|max-min|) of 10^{-3}.
The axial average void fraction and maximum wall temperature distributions are shown in Fig 3. As observed in the result, the overall void fraction is lower in the HCF channel than in the CF channel. This is because the HCF channel has lower local heat flux due to its larger fuel surface area. In addition, given that the same mass flux is used as an inlet flow condition, the HCF channel has a larger coolant mass flow due to its larger flow area. Therefore, it leads to a lower exit void fraction and exit flow quality in the HCF channel. A similar explanation can be applied to the wall temperature distribution in Fig 2 where the wall temperature increases slowly in the HCF channel compared to the cylindrical one. Furthermore, the axial wall temperature in the HCF channel is not monotonically increasing since the twisting fuel geometry results in different cross-sectional configurations along the axial plane which leads to locally different heat removal rates on the wall surface. Lastly, lower void fraction as well as lower wall temperature implies that the HCF channel will have less CRUD which will be explored in future work.

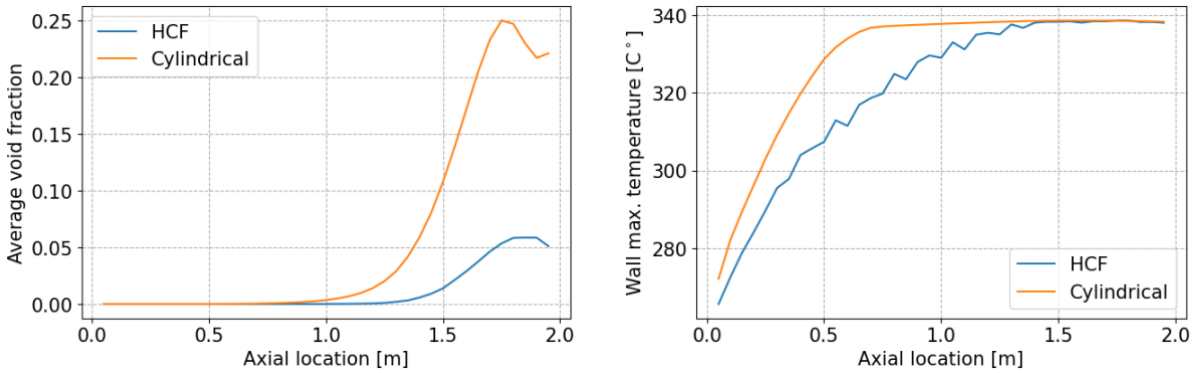

Fig 3. Hot channel analysis result – axial void fraction (left) and wall temperature (right)

3.3 DNB assessment

DNB is a critical phenomenon in pressurized water reactor (PWR) applications since it dominates the reactor safety and can limit the power uprate magnitude which impacts the economics of reactor design. One of the key safety parameters, a Departure from Nucleate Boiling Ratio (DNBR) is defined as the ratio of the heat flux needed to cause DNB to the actual local heat flux and the U.S. Nuclear Regulatory Commission (NRC) requires the minimum DNBR (MDNBR) should be larger than the limit set by the fuel's technical specification at transient overpower for PWR. To investigate a different safety margin in two different channel geometries, numerical boiling tests are carried out by increasing the pin power from the previous hot channel analysis. A DNB occurrence is detected by observing a maximum wall

superheat (T_{sup} =T_{wall} - T_{sat}). In other words, the incremental wall heat flux is applied until a notable temperature excursion is observed.
Fig 4 shows the power ramp-up and wall temperature history during the boiling test in the HCF channel. The result indicates that DNB occurs at a 60 % power increase in the HCF channel and a 32 % increase in the CF channel. Taking the maximum local heat flux at DNB occurrence as a CHF, the MDNBR is evaluated as 1.60 and 1.34 for HCF and CF channels, respectively. Tab 3 summarizes the estimated critical heat flux and MDNBR for both HCF and CF from CFD simulations as well as the estimated values for CF using the Groeneveld CHF look-up table [9] as a reference. As mentioned in the previous discussion, the fuel surface area of HCF is approximately 35 % larger than CF and the local wall heat flux is lower in the HCF channel, accordingly, for the same pin power. In addition, the flow mixing is enhanced by the twisted geometry in the HCF channel which improves heat transfer from the fuel surface. This is confirmed in the lateral velocity profile shown in Fig 5 where the maximum lateral velocity is 40 times larger in the HCF channel at a certain axial plane.

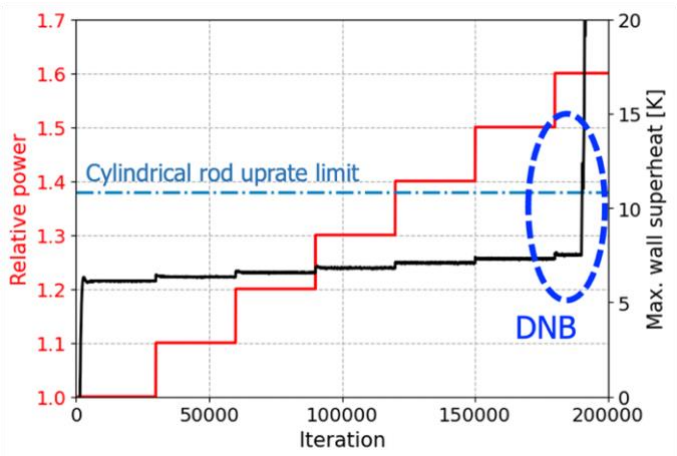

Fig 4. Power ramp-up and wall superheat history in HCF channel boiling test

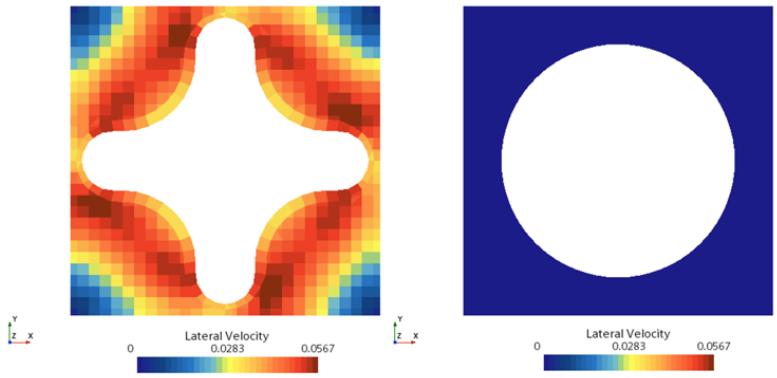

Fig 5. Lateral velocity profile at z=1.5m

	HCF - CFD	CF - CFD	CF - LUT	Unit
Critical heat flux	854.3	963.0	920.1	kW/m^2
MDNBR	1.60	1.34	1.29	-

Tab 3: Comparison of estimated CHF and MDNBR

4. Fuel performance analysis

4.1 Problem setup

In this study, a three-dimensional fuel performance analysis is carried out for a hot fuel pin with a reduced height of 50 cm. The computational mesh is generated using a MOOSE mesh generator which is shown in Fig 6. In BISON modeling, fuel is filled with U-50Zr alloy, cladding is filled with M5 alloy, and displacer material is pure zirconium for the sake of compatibility with the fuel material. The models and parameters used in the BISON simulation are summarized in Tab 4 where the detailed description of each model can be referred to BISON manual [10]. As boundary conditions, zero displacement in the z direction is applied to the bottom plane and the coolant pressure boundary (13.8 MPa) is applied to the entire surface. Lastly, displacements in the lateral direction (x and y) are forced to be zero at the nodes where the fuel rod contacts the neighbouring fuel in the fuel assembly.
A mesh convergence study is performed with a constant average pin power (12.797 kW/m) for 1000 days using five different meshes which are refined in either axial or radial direction. Tab 5 summarizes a few physical quantities including maximum cladding hoop strain and peak fuel temperature at the last time step. In Tab 5, “Z2” means that the mesh is refined twice in the axial direction from the medium mesh. The result shows that the current mesh density (medium) is likely sufficient in this study.

Fig 6. HCF mesh for BISON simulation

Model	Fuel (U-50Zr)	Cladding (M5)	Displacer (pure Zr)
Burnup	UPuZrBurnup	-	-
Thermal properties	INL data [5]	ZryThermal (MATPRO)	ZrThermal
Density (kg/m^3)	9640	6551	6350
Thermal expansion	ComputeDilatation ThermalExpansion FunctionEigenstrain (with INL’s data [5])	ZryThermalExpansion MATPROEigenstrain	ZrThermalExpansion Eigenstrain
Elasticity	UPuZrElasticityTensor	ZryElasticityTensor (MATPRO)	ComputeIsotropic ElasticityTensor
Plasticity	UPuZrPlasticityUpdate Table	ZryPlasticityUpdate (PNNL)	IsotropicPlasticity StressUpdate
Creep	UPuZrCreepUpdate	ZryCreepLimbackHoppe Update	ZrCreepUpdate
Fuel swelling	UPuZrVolumetric SwellingEigenstrain	-	-
Cladding growth	-	ZryIrradiationGrowth Eigenstrain	-
Fission gas release	UPuZrFissionGas Release	-	-

Tab 4: Models and parameters used in BISON simulation of HCF

Mesh	Coarse	Medium	Fine	Z2	Z4	Unit
Max. clad. hoop stress	649	410	424	428	503	MPa
Peak fuel temperature	353	355	354	356	356	°C

Tab 5: Mesh convergence study result

4.2 Metallic fuel model sensitivity

Metallic fuel models in BISON are based on post-irradiation examination data of conventional metallic fuel which is at most 10 wt.% Zr content (U-rich alloy) in mostly α-U phase (α-phase). Therefore, one of the key challenges of fuel performance analysis for Zr-rich metallic fuel like HCF is the validity of using existing models. To investigate the impact of each model on the result, a sensitivity study on metallic fuel models is performed. The peak pin power of 17.877 kW/m is used and adopted from MIT's replica design of the NuScale core and the transient time is 1500 days. Among the metallic fuel models in Tab 4, the models with high uncertainty are chosen as plasticity, creep, and fuel volumetric swelling models. The fission gas release (FGR) model also falls into uncertain models for Zr-rich U-Zr alloy and it calculates the FGR rate as a function of current fuel porosity. Therefore, the FGR model is excluded from the sensitivity study as fuel porosity is affected by other models mentioned above. A sensitivity study is progressed by turning off one of these models at each time and comparing the history of the figure of merits (FOMs) such as von Mises stress and hoop strain.
Fig 7 shows the average cladding von Mises stress and fuel porosity with different model options. When the volumetric swelling model is not used, the cladding stress is underestimated and fuel porosity doesn't change since the fuel swelling is not considered. Regarding inelastic strain models including plastic and creep models, their impact is substantial as shown in a large deviation of both cladding von Mises stress and fuel porosity from the base case. This result is explained by the fact that the strain hardening is not properly captured when the plastic deformation is not considered in the simulation. Therefore, it leads to higher cladding stress due to the exaggerated volume change of the fuel and lower fuel porosity due to larger hydrostatic stress.

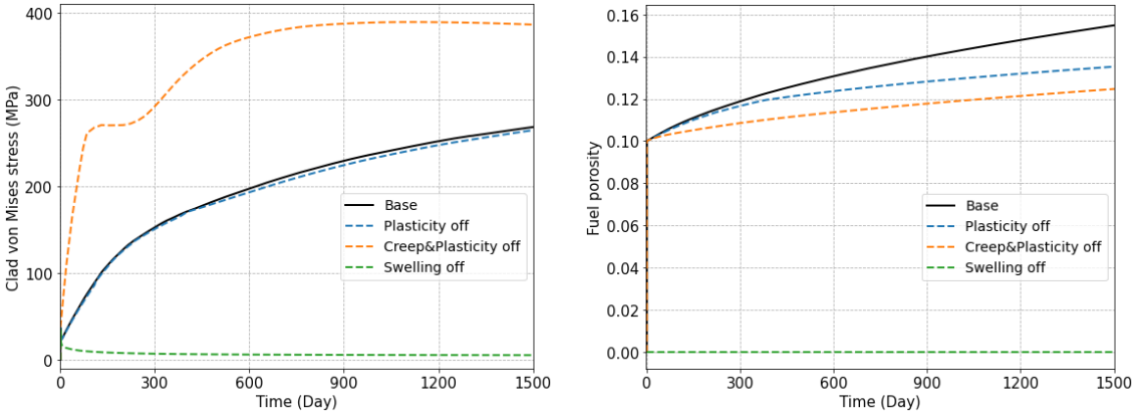

Fig 7. Metallic fuel model sensitivity – cladding von Mises stress (left) and fuel porosity (right)

As an effort to extend the capability of metallic fuel models so that the characteristics of δ-phase U-Zr alloy can be properly captured, the fuel volumetric swelling model is modified. A gaseous swelling in metallic fuel results from anisotropic grain growth of polycrystalline α-phase uranium and it has been shown that the large swelling can be mitigated by reducing the fraction of α-phase [11]. It was observed that the fission gas bubble size in U-40Zr alloy (δ-phase) is around 6nm while it is 70 nm in U-0.1Zr alloy (α-phase) after the same dose of 140-keV helium ion-beam irradiation [12]. Based on this experimental observation, a fission gas bubble radius is added as an input parameter of the fuel swelling model to reflect the difference in fission gas bubble size depending on the phase. The fission gas bubble radius is fixed as

10 nm for HCF modeling based on [12]. Fig 8 shows the maximum von Mises stress and the FGR rate with different fission gas bubble sizes. It is confirmed that the smaller the bubble radius is, the smaller the cladding stress is due to the less gaseous swelling of the fuel. Furthermore, with a bubble radius of 10 nm, fission gas is not released during the fuel lifetime, which is one of the strengths of HCF using Zr-rich alloy. It is worth mentioning that this model should be further improved when the neutron irradiation test result becomes available for U-50Zr alloy.

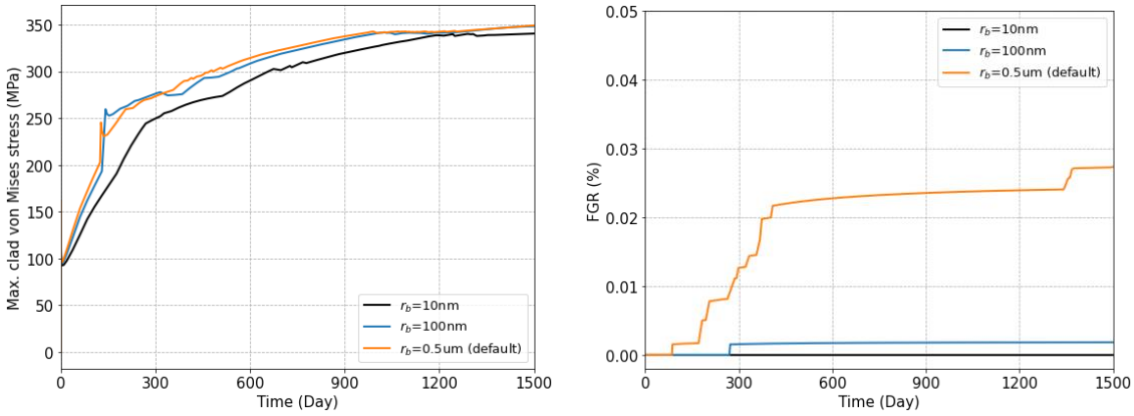

Fig 8. Max. clad von Mises stress (left) FGR rate (right) with different fission gas bubble sizes

4.3 Hot fuel pin analysis

To investigate the thermo-mechanical behaviour of metallic HCF under the most limiting conditions during normal operation, a hot fuel pin analysis is carried out for a 25 cm height HCF rod. Fig 9 shows the linear power history and the axial peaking factors of the hot fuel pin, referenced from MIT's replica design of the NuScale core. The transient time is 1577 days which is a fuel lifetime in NuScale core and the simulation setup including mesh, models, and boundary conditions are identical as aforementioned.

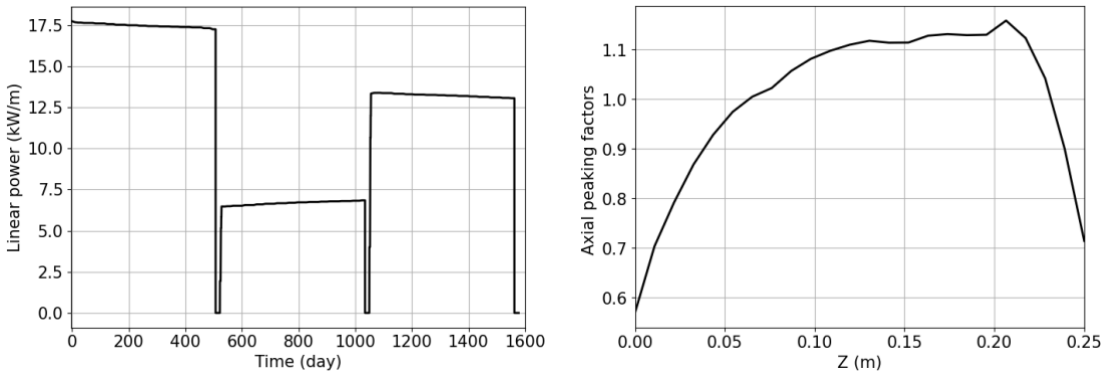

Fig 9. Linear power history (left) and axial peaking factors (right) of the hot fuel pin

As shown in the contour of von Mises stress at the beginning of life (BOL) and end of life (EOL) of the fuel in Fig 10, stress is concentrated at contact points and valley regions. Since the zero displacement boundary conditions are applied at contact points as constraints provided by the neighbouring fuels, cladding at these points shows relatively higher stress. The higher stress in valley regions is due to the force exerted by fuel swelling. Furthermore, the fuel volume has increased by around 10 % at EOL and this volumetric swelling may reduce the flow area. Therefore, the future study will include the impact of flow blockage due to fuel swelling on the safety performance of HCF.

Lastly, hot fuel pin analysis is also carried out for UO_2 CF in two-dimensional axisymmetric geometry for comparison with metallic HCF. Fig 11 shows the comparison result for peak fuel

temperature and maximum cladding von Mises stress. Additionally, a one-to-one comparison of the major FOMs at EOL is listed in Tab 6. HCF shows a very low operating temperature compared to UO_2 fuel due to the high thermal conductivity of metallic alloy. However, HCF is relatively susceptible regarding the structural integrity of cladding due to a large volumetric swelling of metallic fuel compared to ceramic fuel. The maximum cladding stress of U-50Zr HCF is estimated as 409 MPa which is lower than 491 MPa which was reported as the yield strength of irradiated M5 alloy [13].

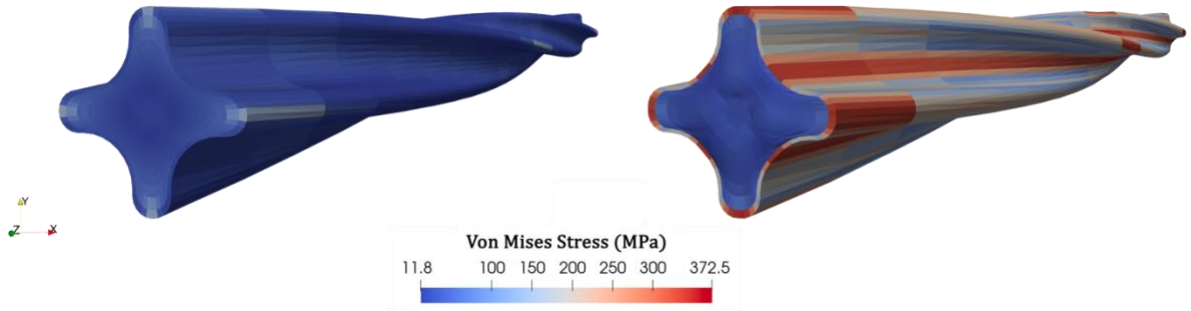

Fig 10. Hot fuel pin von Mises stress history – BOL (left) and EOL (right)

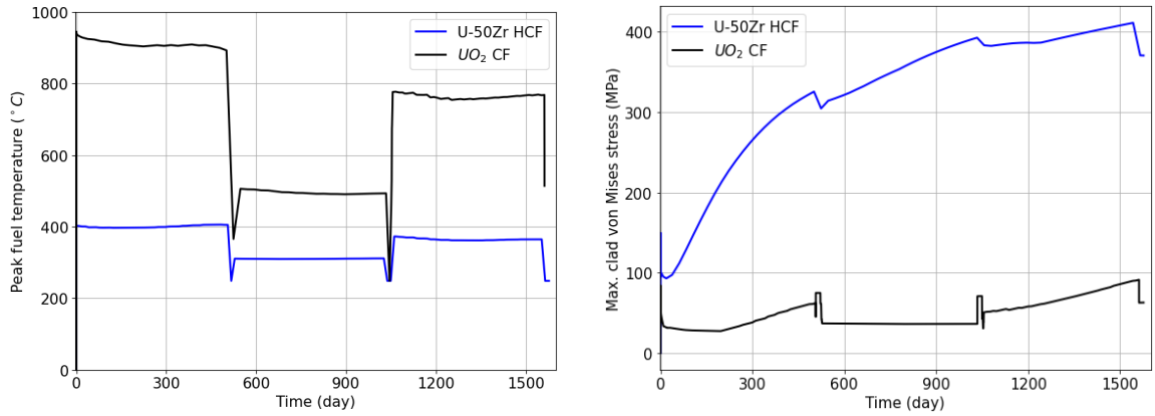

Fig 11. Comparison of U-50Zr HCF and UO_2 CF – Peak fuel temperature (left) and maximum cladding von Mises stress (right)

	U-50Zr HCF	**UO_2 CF**	**Unit**
Max. cladding stress	409	91	MPa
Max. cladding total hoop strain	0.035	0.002	-
Max. cladding plastic hoop strain	0.003	0	-
Peak fuel temperature	357	1231	°C

Tab 6: Comparison with UO2 CF at EOL

5. Conclusion

As a fundamental design study on utilizing metallic HCF in light-water cooled SMRs, the safety and thermo-mechanical performance of HCF with U-50Zr alloy is investigated. In the safety performance study using the Eulerian-based two-fluid approach, hot channel analysis and DNB assessment are carried out. With the same power and inlet mass flux conditions, an HCF channel shows better heat removal capability which can be found in lower exit void fraction and lower wall temperature. Furthermore, an HCF channel shows higher MDNBR compared to a cylindrical channel which indicates that HCF geometry is expected to have room for a power uprate to achieve a comparable safety performance with cylindrical rod geometry.

In the thermo-mechanical performance study, a sensitivity study on metallic fuel models in BISON is performed to see the impact of each model on the simulation result. In particular, the fuel volumetric swelling model is improved to capture different fission gas behaviour in Zr-rich U-Zr alloy. Lastly, through hot fuel pin analysis, main FOMs including maximum cladding stress and peak fuel temperature are compared with cylindrical UO_2 fuel under the same operating conditions. Due to the characteristics of metallic fuel such as high thermal conductivity and large swelling during irradiation, HCF shows a much lower fuel operating temperature but higher cladding stress.

Given that HCF rods are self-spacing by supporting each other at every twist pitch, future work related to fuel performance analysis will include contact mechanics through multiple rods modeling to investigate the structural integrity of HCF at contact points. Furthermore, coupling analysis between CFD and fuel performance code will be of great interest which enables further exploration of multi-physics problems such as the impact of coolant blockage due to fuel swelling.

6. Acknowledgment

This study is supported by the Nuclear Energy University Program (NEUP) of the U.S. Department of Energy (Contract number: DE-NE0009273). The authors would like to thank Professor Emilio Baglietto at MIT NSE for providing access to the STAR-CCM+, a graduate student Assil Halimi at MIT NSE for providing a reference MIT replica design of NuScale core supported under the same NEUP grant, and Guillaume Giudicelli at Idaho National Lab (INL) for supporting the use of MOOSE framework. This research made use of INL's High Performance Computing systems located at the Collaborative Computing Center and supported by the Office of Nuclear Energy of the U.S. Department of Energy and the Nuclear Science User Facilities under Contract No. DE-AC07-05ID14517.

7. References

[1] J. Malone, A. Totemeier, N. Shapiro, and S. Vaidyanathan, "Lightbridge Corporation's Advanced Metallic Fuel for Light Water Reactors," *Nuclear Technology*, vol. 180, no. 3, pp. 437–442, Dec. 2012, doi: 10.13182/NT12-A15354.

[2] Y. Choi and K. Shirvan, "Assessment of NuScale SMR Core Design with Helical Cruciform Fuel Rods," presented at the International Congress on Advances in Nuclear Power Plants (ICAPP), Gyeongju, Republic of Korea, 2023.

[3] Simens, "Simcenter STAR-CCM+ 2210 User Guide." 2022.

[4] R. L. Williamson *et al.*, "Multidimensional multiphysics simulation of nuclear fuel behavior," *Journal of Nuclear Materials*, vol. 423, no. 1–3, pp. 149–163, Apr. 2012, doi: 10.1016/j.jnucmat.2012.01.012.

[5] G. Beausoleil *et al.*, "U-50Zr Microstructure and Property Assessment for LWR Applications," INL/EXT21-64614, 1825221, Sep. 2021. doi: 10.2172/1825221.

[6] H. Okamoto, "U-Zr (Uranium-Zirconium)," *J Phs Eqil and Diff*, vol. 28, no. 5, pp. 499–500, Oct. 2007, doi: 10.1007/s11669-007-9155-1.

[7] K. Shirvan, "Numerical investigation of the boiling crisis for helical cruciform-shaped rods at high pressures," *International Journal of Multiphase Flow*, vol. 83, pp. 51–61, Jul. 2016, doi: 10.1016/j.ijmultiphaseflow.2016.03.014.

[8] S. J. Kim, R. C. Johns, J. Yoo, and E. Baglietto, "Progress Toward Simulating Departure from Nucleate Boiling at High-Pressure Applications with Selected Wall Boiling Closures," *Nuclear Science and Engineering*, vol. 194, no. 8–9, pp. 690–707, Sep. 2020, doi: 10.1080/00295639.2020.1743579.

[9] D. C. Groeneveld *et al.*, "The 2006 CHF look-up table," *Nuclear Engineering and Design*, vol. 237, no. 15–17, pp. 1909–1922, Sep. 2007, doi: 10.1016/j.nucengdes.2007.02.014.

[10] J. D. Hales *et al.*, "BISON Theory Manual The Equations behind Nuclear Fuel Analysis," INL/EXT-13-29930 Rev. 3, Sep. 2016. doi: 10.2172/1374503.

[11]G. L. Hofman, R. G. Pahl, C. E. Lahm, and D. L. Porter, “Swelling behavior of U-Pu-Zr fuel,” *Metall Trans A*, vol. 21, no. 2, pp. 517–528, Feb. 1990, doi: 10.1007/BF02671924.
[12]S. Ahn, S. Irukuvarghula, and S. M. McDeavitt, “Microstructure of α-U and δ-UZr2 phase uranium–zirconium alloys irradiated with 140-keV He+ ion-beam,” *Journal of Alloys and Compounds*, vol. 681, pp. 6–11, Oct. 2016, doi: 10.1016/j.jallcom.2016.04.219.
[13]B. Cazalis *et al.*, “The PROMETRA Program: Fuel Cladding Mechanical Behavior under High Strain Rate,” *Nuclear Technology*, vol. 157, no. 3, pp. 215–229, Mar. 2007, doi: 10.13182/NT07-A3814.